

Efficient Reliability Analysis using Generalized Multifidelity Modeling and Explainable Active Learning

Promit Chakroborty

Graduate Student, Dept. of Civil and Systems Engg., Johns Hopkins University, Baltimore, U.S.A.

Somayajulu L. N. Dhulipala

Computational Scientist, Idaho National Laboratory, Idaho Falls, U.S.A.

Michael D. Shields

Associate Professor, Dept. of Civil and Systems Engg., Johns Hopkins University, Baltimore, U.S.A.

ABSTRACT: To assess the reliability of critical engineering systems like nuclear plants and infrastructure systems and improve the robustness of design, engineers have to quantify the uncertainties surrounding the system behavior accurately. However, the complexity of the problem can make standard reliability analysis algorithms prohibitively expensive, primarily due to the high computational cost of estimating the system response at each iteration. This cost can be greatly reduced by using multi-fidelity modeling and machine learning to build a surrogate model to replace the expensive response function. We propose a general and robust method for building surrogates from multiple Low Fidelity (LF) models coupled with machine learning to retain accuracy. Our framework first constructs “Corrected Low Fidelity models” (CLFs) by coupling a High Fidelity (HF) model inferred Gaussian Process correction term with each of the LF models. It then uses the correction terms to assign model probabilities to each of these CLFs in an explainable way before using them to assemble the final surrogate. No assumptions are made about the type of the LF models or their correlation with the HF model. The proposed surrogate modeling framework is used within the subset simulation algorithm (a variance-reduced MCMC-based reliability analysis algorithm) for enhanced efficiency. Additionally, an active learning step is added to the algorithm to adaptively decide when the surrogate is not sufficiently accurate, at which point the HF model is called and used to refine the surrogate. Through a frame buckling example, our method is shown to be highly efficient at reducing the expensive HF model calls while accurately estimating the failure probability.

1. INTRODUCTION

Estimating the failure probability is an essential component of the risk assessment and design of a structural system. Theoretically, this is done by estimating the following integral

$$P_f = \int_{\mathbf{x} \in \Omega_F} q(\mathbf{x}) dx = \int_{\mathbf{x} \in \Omega} I_{\Omega_F}(\mathbf{x}) q(\mathbf{x}) dx, \quad (1)$$

where \mathbf{x} is a random vector of the system’s uncertain parameters having joint probability density

$q(\mathbf{x})$, and Ω is the set of all possible system states. $\Omega_F = \{\mathbf{x} : I_{\Omega_F}(\mathbf{x}) = 1\}$, where the indicator function $I_{\Omega_F}(\mathbf{x})$ equals 1 for states \mathbf{x} that correspond to failure and is 0 otherwise. To determine failure for a given \mathbf{x} , we evaluate the performance function $g(\mathbf{x})$; $g(\mathbf{x}) \leq F$ corresponds to failure, where F is a pre-defined failure threshold. This integral is analytically intractable for most cases, and therefore, simulation methods are used to estimate it (such

as Monte Carlo or various variance-reduced Monte Carlo, e.g., Importance Sampling, Control Variates, or Subset Simulation). However, for most real-world structures, evaluating $g(\mathbf{x})$ is highly computationally expensive, making even simulation methods impractical. In such cases, surrogate modeling techniques need to be explored, which replace the expensive $g(\mathbf{x})$ with a cheaper approximation.

There are broadly two ways to build a surrogate. One is to use fast-running data-driven approaches (active learning) to approximate the response, such as Polynomial Chaos Expansions (Schöbi and Sudret (2014)), Neural Networks (Papadrakakis et al. (1996)), or Gaussian Process Regression (GPR) (Bichon et al. (2008); Echard et al. (2011)). The other method is to incorporate information from multiple levels of fidelity (multifidelity modeling), where the Low Fidelity (LF) models are less accurate but cheaper than the High Fidelity (HF) models. This is done using statistical tools like Control Variates (Gorodetsky et al. (2020)) or Importance Sampling (Kramer et al. (2019)). Methods that couple multifidelity modeling with active learning have also been explored (Zhang et al. (2022)).

In this paper, we present a surrogate modeling framework that combines information from N LF models to build a robust and explainable surrogate for the target HF model. Gaussian Process Regression is used to recover the accuracy lost by using LF models, and an on-the-fly sufficiency check is incorporated to ensure that the surrogate is updated whenever the accuracy falls below a pre-defined threshold. Finally, the surrogate is used within a Subset Simulation sampling scheme to build the proposed Low Fidelity Model Combination (LFMC) algorithm, which is shown to estimate small failure probabilities efficiently.

2. THEORY & METHODOLOGY

2.1. Background

2.1.1. Subset Simulation (SuS)

Subset Simulation, introduced in Au and Beck (2001), is a variance reduction technique in which a small target failure probability is estimated as the product of larger intermediate failure probabilities, thereby improving the efficiency of the process. This is achieved by constructing a sequence of

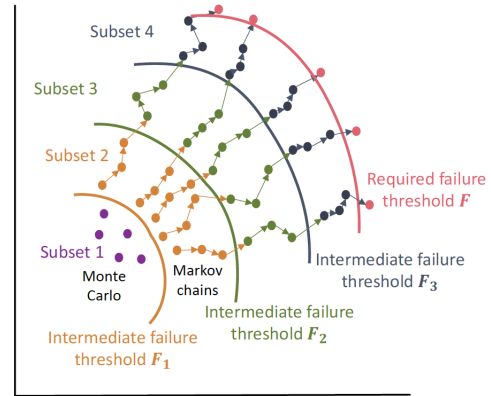


Figure 1: Visualization of Subset Simulation (adapted from Figure 7 in Dhulipala et al. (2022))

nested subsets $S_1 \supset S_2 \supset \dots \supset S_{N_s}$ with associated intermediate failure thresholds $F_1 < F_2 < \dots < F_{N_s}$, such that the first subset (S_1) coincides with the full sampling domain, and the intermediate failure thresholds converge to the true failure threshold F , i.e., $F_{N_s} = F$. Here, N_s is the total number of subsets. As shown in Figure 1, the intermediate failure threshold for subset $s - 1$ forms the boundary for subset s .

Each intermediate failure probability $P_{s|s-1}$ is defined as the probability that a sample drawn from subset S_{s-1} also lies in subset S_s , i.e., a point from S_{s-1} crosses F_{s-1} . P_1 is defined similarly with respect to S_1 and F_1 . Thus, the target failure probability is calculated as

$$P_f = P_1 \prod_{s=2}^{N_s} P_{s|s-1}, \quad (2)$$

Often the intermediate failure thresholds are set adaptively by selecting a target intermediate failure probability and constructing the threshold such that the intermediate probability matches this target.

2.1.2. Gaussian Process Regression (GPR)

Gaussian Process Regression is a numerical modeling technique that uses a given set of observations of a function to predict the function response at any non-observed point and specifies a Gaussian distribution centered at the predicted value to model the uncertainty associated with the prediction. This is done by approximating the target function ($g(\mathbf{x})$) as the realization of a Gaussian Process ($\mathcal{G}(\mathbf{x})$) with

chosen covariance kernel K . For a set of observed points $\mathbf{X} = \{\mathbf{x}_1, \mathbf{x}_2, \dots, \mathbf{x}_n\}$ with observations $g(\mathbf{X})$, the Gaussian distribution associated with the predicted response of a “new” point \mathbf{x}^* is given by

$$\begin{aligned} \mathcal{G}(\mathbf{x}^*) &\sim \mathcal{N}(\boldsymbol{\mu}_{\mathcal{G}}(\mathbf{x}^*), \boldsymbol{\sigma}_{\mathcal{G}}(\mathbf{x}^*)) \\ \boldsymbol{\mu}_{\mathcal{G}}(\mathbf{x}^*) &= K(\mathbf{x}^*, \mathbf{X}) K(\mathbf{X}, \mathbf{X})^{-1} g(\mathbf{X}) \\ \boldsymbol{\sigma}_{\mathcal{G}}(\mathbf{x}^*) &= K(\mathbf{x}^*, \mathbf{x}^*) \\ &\quad - K(\mathbf{x}^*, \mathbf{X}) K(\mathbf{X}, \mathbf{X})^{-1} K(\mathbf{X}, \mathbf{x}^*) \end{aligned} \quad (3)$$

where $K(\mathbf{X}, \mathbf{X})$ denotes the block matrix whose (i, j) th element is $K(\mathbf{x}_i, \mathbf{x}_j)$ such that $\mathbf{x}_i, \mathbf{x}_j \in \mathbf{X}$, and $K(\mathbf{X}, \mathbf{x}^*)$ and $K(\mathbf{x}^*, \mathbf{X})$ denote similar block matrices (Rasmussen and Williams (2005)). To fully specify K , the required hyperparameters are learned by minimizing the negative marginal log-likelihood \mathcal{L} , where

$$\begin{aligned} \mathcal{L} &\propto \frac{1}{2} \log |K(\mathbf{X}, \mathbf{X})| \\ &\quad + \frac{1}{2} (g(\mathbf{X}))^T K(\mathbf{X}, \mathbf{X})^{-1} g(\mathbf{X}) \end{aligned} \quad (4)$$

2.2. Theory

2.2.1. Surrogate Formulation and Assembly

The surrogate is formed by adding a GP correction term to each LF model and assembling the corrected predictions. Thus, for each LF model $L_i(\bar{\mathbf{x}})$, $i \in \{1, 2, \dots, N\}$, a Corrected Low Fidelity (CLF) model $S_i(\bar{\mathbf{x}})$ is formed by applying an independent GP correction term $G_i(\bar{\mathbf{x}})$ that models the difference between L_i and H , i.e.,

$$S_i(\bar{\mathbf{x}}) = L_i(\bar{\mathbf{x}}) + G_i(\bar{\mathbf{x}}), \quad \forall i \in \{1, 2, \dots, N\} \quad (5)$$

Here, $\bar{\mathbf{x}}$ denotes the vector of all inputs. The GP correction terms are also used to assign a local model probability $p_i(\bar{\mathbf{x}})$ to each CLF. This is done based on the hypothesis that the “best” model is the one that has the greatest probability of being closest to the HF model (i.e., it has the smallest correction $|G_i(\bar{\mathbf{x}})|$). If L_i has associated local cost $\tau_i(\bar{\mathbf{x}})$, then a cost-biasing function $\gamma(\tau_i(\bar{\mathbf{x}}))$ can be constructed, and the cost-biased correction (i.e., $\gamma(\tau_i(\bar{\mathbf{x}}))|G_i(\bar{\mathbf{x}})|$) is considered instead. Thus, $p_i(\bar{\mathbf{x}})$ is the probability that $S_i(\bar{\mathbf{x}})$ has the smallest cost-biased correction.

This can be calculated as

$$p_i(\bar{\mathbf{x}}) = \int_0^\infty \left[f_i(z) \prod_{j \neq i} \{1 - F_j(z)\} \right] dz \quad (6)$$

where $j \in \{1, 2, \dots, N\}$

$$f_i(z) = \frac{\left[\exp\left(-\frac{(z - \mu_i(\bar{\mathbf{x}}))^2}{2\sigma_i^2(\bar{\mathbf{x}})}\right) + \exp\left(-\frac{(z + \mu_i(\bar{\mathbf{x}}))^2}{2\sigma_i^2(\bar{\mathbf{x}})}\right) \right]}{\sigma_i(\bar{\mathbf{x}}) \sqrt{2\pi}} \quad (7)$$

$$F_i(z) = \frac{1}{2} \left[\operatorname{erf}\left(\frac{z - \mu_i(\bar{\mathbf{x}})}{\sqrt{2}\sigma_i(\bar{\mathbf{x}})}\right) + \operatorname{erf}\left(\frac{z + \mu_i(\bar{\mathbf{x}})}{\sqrt{2}\sigma_i(\bar{\mathbf{x}})}\right) \right] \quad (8)$$

$$\operatorname{erf}(z) = \frac{2}{\sqrt{\pi}} \int_0^z e^{-t^2} dt \quad (9)$$

where $\mu_i(\bar{\mathbf{x}}) = \gamma(\tau_i(\bar{\mathbf{x}}))E[G_i(\bar{\mathbf{x}})]$ and $\sigma_i(\bar{\mathbf{x}}) = \gamma(\tau_i(\bar{\mathbf{x}}))\sqrt{\operatorname{Var}[G_i(\bar{\mathbf{x}})]}$. A detailed derivation of Equation 6 is presented in Chakroborty et al. (2022), along with deeper discussions about the method.

Once the probabilities have been calculated, they are used to assemble the CLFs into the final surrogate $S(\bar{\mathbf{x}})$. Three assembly methods have been considered here: Low Fidelity Model Averaging (LFMA), Low Fidelity Deterministic Selection (LFDS), and Low Fidelity Stochastic Selection (LFSS). These assembly procedures are defined as

$$S(\bar{\mathbf{x}}) = \begin{cases} \sum_{i=1}^N p_i(\bar{\mathbf{x}}) S_i(\bar{\mathbf{x}}) & \text{LFMA} \\ S_k(\bar{\mathbf{x}}) \text{ s.t. } p_k(\bar{\mathbf{x}}) = \max\{p_i(\bar{\mathbf{x}})\} & \text{LFDS} \\ S_k(\bar{\mathbf{x}}) \text{ with probability } p_k(\bar{\mathbf{x}}) & \text{LFSS} \end{cases} \quad (10)$$

Note that the LF models and the HF model need not have the same set of inputs. In the general case, the vector of inputs for L_i can be termed $\bar{\mathbf{x}}_{L_i}$ and that for H can be called $\bar{\mathbf{x}}_H$. Then, $\bar{\mathbf{x}} = \{\cup_{i=1}^N \bar{\mathbf{x}}_{L_i}\} \cup \bar{\mathbf{x}}_H$.

2.2.2. On-the-fly Sufficiency Check

This active learning strategy is adapted from the U learning function developed by Echard et al. (2011) and integrated into SuS for reliability analysis. At each point $\bar{\mathbf{x}}$, the subset-dependent U function is calculated, which is defined as

$$U_s(\bar{\mathbf{x}}) = \frac{|S(\bar{\mathbf{x}}) - F_s|}{\sigma(\bar{\mathbf{x}})} \quad (11)$$

where s is the subset index and F_s is the corresponding failure threshold. $S(\bar{\mathbf{x}})$ is the assembled surrogate model (Eq. (10)), and $\sigma(\bar{\mathbf{x}})$ is the associated standard deviation at $\bar{\mathbf{x}}$, which can be calculated by noting that the surrogate at a point is a Gaussian (for LFDS/LFSS) or a linear combination of Gaussians (for LFMA) (Eq. (10)). If $U_s \leq U_T$ (a predefined threshold usually taken to be 2), then the surrogate is deemed insufficient. In this case, $H(\bar{\mathbf{x}})$ replaces $S(\bar{\mathbf{x}})$ as the predicted response at $\bar{\mathbf{x}}$, and the surrogate is refined. This refinement is described in more detail in section 2.3.

2.3. Methodology

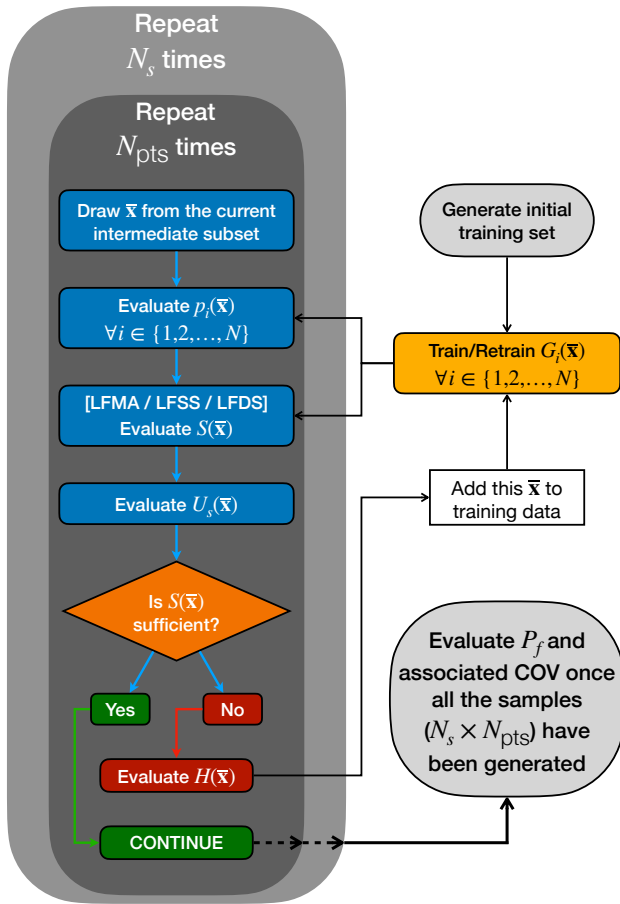


Figure 2: LFMC Algorithm Flowchart.

The Low Fidelity Model Combination (LFMC) algorithm utilizes the formulation described above to build a surrogate that approximates the target response function for use within a SuS sampling scheme to conduct reliability analysis efficiently.

First, a small number of samples are generated; all the models (LFs and HF) are evaluated at these points, and all GP correction terms are trained with this as the initial training data. After this, samples are generated in accordance with the SuS framework, with the LFMC surrogate being used to estimate the response. In each subset, a total of N_{pts} sample points are generated. For each new sample point, first, all the GP correction terms are evaluated for both the mean prediction and the standard deviation. These are used to assign the model probabilities for each CLF at that point (Eq. 6). Then the surrogate is evaluated: If the LFMA assembly scheme is used, all the LF models need to be evaluated, but if LFDS/LFSS is used, only the selected LF model needs to be evaluated for the surrogate (Eq. 10). Once the surrogate response has been evaluated, the subset-dependent U value is evaluated (Eq. 11). (The standard deviation of the surrogate is also necessary to compute at this point.) The intermediate failure probability required for the U value is computed as the $\tilde{\pi}^{\text{th}}$ quantile of the system responses of the samples generated within the subset thus far, where $\tilde{\pi}$ is the pre-selected target intermediate failure probability per Au and Beck (2001). If the response is found to be insufficiently accurate, the HF model is evaluated, and the point is added to the training data for the associated GP correction term/terms to be refined. The final subset ($s = N_s$) is reached when the $\tilde{\pi}^{\text{th}}$ quantile of the system responses $\leq F$, and here the U_s value is calculated using $F_{N_s} = F$, the true failure threshold. Figure 2 presents a simplified flowchart for the algorithm.

Once all the points are generated, the following estimators can be used to estimate each intermediate failure probability, which are combined according to Eq. 2 into the final failure probability.

$$P_1 = \frac{1}{N_{pts}} \sum_{l=1}^{N_{pts}} \mathcal{P}_l^{(1)} \quad (12)$$

$$P_{s|s-1} = \frac{1}{N_{pts}} \sum_{l=1}^{N_{pts}} \mathcal{P}_l^{(s)}, \forall s = \{2, 3, \dots, N_s\} \quad (13)$$

$$\mathcal{P}_l^{(s)} = \begin{cases} \Phi(U_s(\bar{\mathbf{x}}_l)) & \text{if } I_{F_s, S}(\bar{\mathbf{x}}_l) = 1 \\ \Phi(-U_s(\bar{\mathbf{x}}_l)) & \text{if } I_{F_s, S}(\bar{\mathbf{x}}_l) = 0 \end{cases} \quad (14)$$

The coefficient of variation (COV) estimator is presented in Chakroborty et al. (2022), along with the derivations for both estimators.

3. EXAMPLE APPLICATION

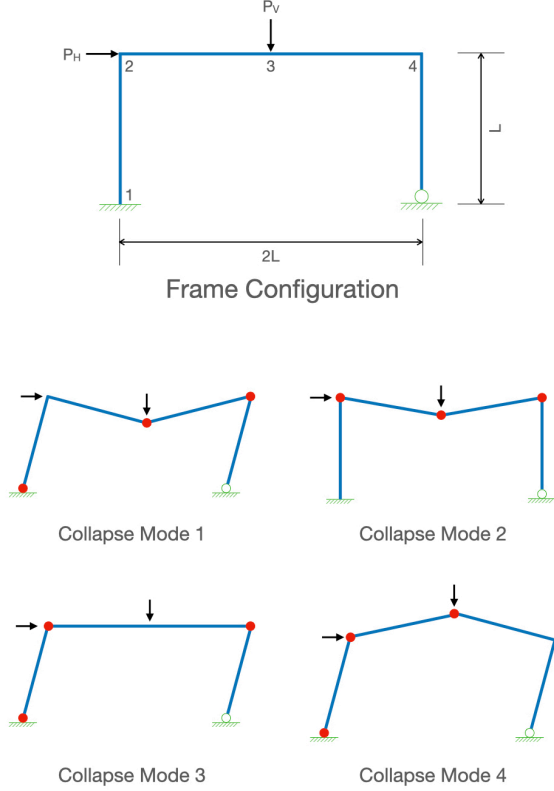


Figure 3: An illustration of the frame configuration and associated collapse modes.

To showcase the performance of our algorithm, we apply it to an analytical rigid-plastic portal frame example adapted from Xu et al. (2022). Figure 3 depicts the frame subjected to vertical and horizontal loads P_V and P_H as well as its possible collapse modes. Failure occurs when any one of the collapse modes occurs; the corresponding response function can be written as

$$g(\bar{\mathbf{x}}) = \min \begin{cases} M_1 + 2M_3 + 2M_4 - P_H - P_V \\ M_2 + 2M_3 + M_4 - P_V \\ M_1 + M_2 + M_4 - P_H \\ M_1 + 2M_2 + 2M_3 - P_H + P_V \end{cases} \quad (15)$$

where M_1, M_2, M_3, M_4 are the moment capacities at the plastic hinges formed at points 1, 2, 3, 4,

respectively (as shown in Figure 3), and $\bar{\mathbf{x}} = \{M_1, M_2, M_3, M_4, P_H, P_V\}$. The response function itself is the HF model, while each of the four individual collapse modes is taken as LF models L_1, L_2, L_3 , and L_4 . Two cases are considered: (a) A 6-D case, where all four moment capacities and both load variables are taken as random variables, and (b) A 2-D case, where the moment capacities are constants and only the load variables are stochastic. Table 1 lists the variables for both cases.

Variable	6-D Case	2-D Case
	Distribution	Value/Distribution
M_1	$\mathcal{N}(1.0, 0.15)$	1.0
M_2	$\mathcal{N}(1.0, 0.15)$	1.0
M_3	$\mathcal{N}(1.0, 0.15)$	1.0
M_4	$\mathcal{N}(1.0, 0.15)$	1.0
P_H	$\mathcal{N}(1.5, 0.45)$	$\mathcal{N}(0.0, 1.0)$
P_V	$\mathcal{N}(1.5, 0.45)$	$\mathcal{N}(0.0, 1.0)$

Table 1: List of Random Variables. (\mathcal{N} represents a Gaussian random variable, with parameters mean and standard deviation, respectively.)

Quantity	Method	Value
P_f (COV)	6-D SuS	5.94E-3 (0.13)
	6-D LFMA	7.15E-3 (0.14)
	6-D LFDS	5.56E-3 (0.13)
	6-D LFSS	7.12E-3 (0.13)
# HF Calls (% of total)	6-D SuS	6000 (100%)
	6-D LFMA	357 (5.95%)
	6-D LFDS	227 (3.78%)
R^2 Value	6-D LFSS	298 (4.97%)
	6-D LFMA	0.9949
	6-D LFDS	0.9894
	6-D LFSS	0.9948

Table 2: Results for 6-D Case. (6000 total samples generated for each method.)

Tables 2 and 3 compare the failure probability calculated by the LFMC algorithm to that calculated by Subset Simulation (for both cases) and Crude Monte Carlo (CMC) (for the 2-D case only). The results clearly show that LFMC is able to accurately estimate the failure probabilities to a comparable coefficient of variation (COV) level using

Quantity	Method	Value
P_f (COV)	2-D CMC	1.60E-3 (0.025)
	2-D SuS	1.22E-3 (0.056)
	2-D LFDS	1.64E-3 (0.059)
# HF Calls (% of total)	2-D CMC	1E6 (100%)
	2-D SuS	60,000 (100%)
	2-D LFDS	245 (0.41%)
R^2 Value	2-D LFDS	0.9961

Table 3: Results for 2-D Case. (60,000 total samples generated for SuS and LFDS, 1 million samples generated for Crude Monte Carlo (CMC).)

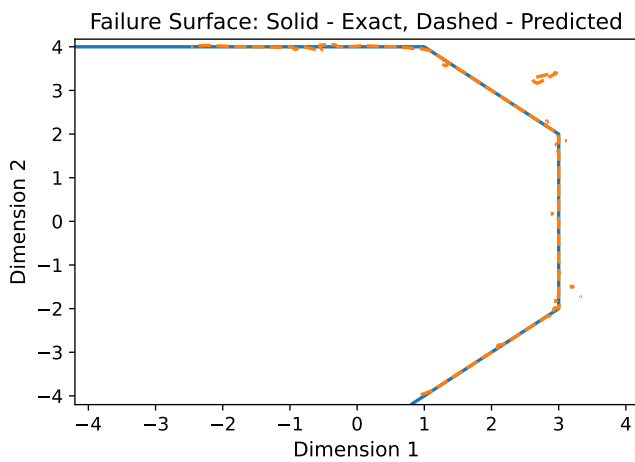


Figure 4: Comparison between exact failure boundary and failure boundary predicted by the LFMC - LFDS surrogate for the 2-D case.

only a small fraction of HF calls compared to SuS or CMC. Figure 4 shows that the surrogate built by LFMC can accurately capture the failure surface. This is supported by the R^2 values presented, which prove that the surrogates are excellent approximations of the target response function. Figure 5 illustrates the explainability of the probability assignment scheme: in LFDS the LF model with the maximum probability is selected, and the surrogate is clearly calling the LF model associated with the nearest collapse mode limit surface. Note that for regions far away from any of the collapse mode limit surfaces, the model selection is not as accurate. This is because the algorithm does not prioritize the accuracy of the surrogate in these regions, as they are not important for predicting fail-

ure. Thus, the GP correction terms are not refined for these regions, which decreases the accuracy of the probability assignment.

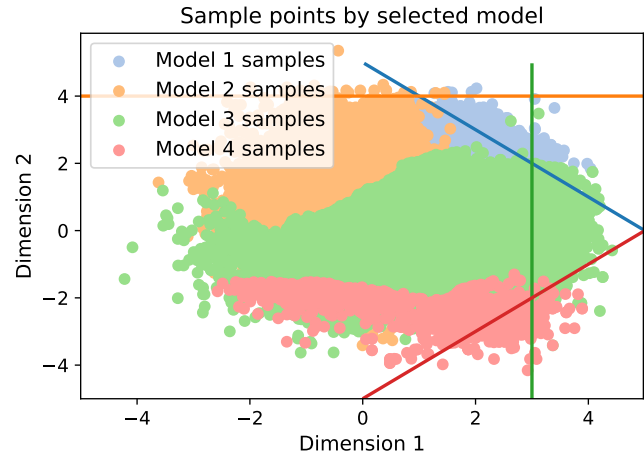


Figure 5: Samples drawn by LFMC - LFDS colored by LF model call. Initial training set is removed. The contour of the failure surface is added, with each branch color-coded to the corresponding LF model.

4. CONCLUSIONS

Reliability analysis is often infeasible for real-world problems due to the large computational cost of evaluating the system response using highly accurate HF models. To circumvent this issue, less accurate but cheaper LF models or data-driven machine-learned regression models can be used to estimate the system response. We present here a general surrogate modeling framework that combines information from multiple LF models in an explainable and robust way, and couples it with GP correction terms to recover accuracy. The method makes no assumptions about the relationships between the LF models and is shown to be accurate and highly efficient - reducing the number of HF model calls necessary by ~ 2 orders of magnitude compared to standard SuS. Further, the variance associated with the algorithm's predictions is similar to standard SuS, and the surrogate created by the method closely mimics the target response function. The algorithm has been shown to work for moderate dimensionality. However, since GPs are used for the correction terms and the probability calculation, LFMC suffers from the same draw-

backs as does GPR: for high-dimensional problems, the efficiency is greatly reduced, as the GPs will require large amounts of data to be sufficiently trained.

5. REFERENCES

- Au, S. K. and Beck, J. L. (2001). “Estimation of small failure probabilities in high dimensions by subset simulation.” *Probabilistic Engineering Mechanics*, 16(4), 263–277.
- Bichon, B. J., Eldred, M. S., Swiler, L. P., Mahadevan, S., and McFarland, J. M. (2008). “Efficient global reliability analysis for nonlinear implicit performance functions.” *AIAA Journal*, 46, 2459–2468.
- Chakroborty, P., Dhulipala, S. L. N., Che, Y., Jiang, W., Spencer, B. W., Hales, J. D., and Shields, M. D. (2022). “General multi-fidelity surrogate models: Framework and active learning strategies for efficient rare event simulation, <<https://arxiv.org/abs/2212.03375>>.”
- Dhulipala, S. L. N., Jiang, W., Spencer, B. W., Hales, J. D., Shields, M. D., Slaughter, A. E., Prince, Z. M., Labouré, V. M., Bolisetti, C., and Chakroborty, P. (2022). “Accelerated statistical failure analysis of multifidelity TRISO fuel models.” *Journal of Nuclear Materials*, 563.
- Echard, B., Gayton, N., and Lemaire, M. (2011). “AK-MCS: An active learning reliability method combining Kriging and Monte Carlo Simulation.” *Structural Safety*, 33(2), 145–154.
- Gorodetsky, A. A., Geraci, G., Eldred, M. S., and Jake-man, J. D. (2020). “A generalized approximate control variate framework for multifidelity uncertainty quantification.” *Journal of Computational Physics*, 408.
- Kramer, B., Marques, A. N., Peherstorfer, B., Villa, U., and Willcox, K. (2019). “Multifidelity probability estimation via fusion of estimators.” *Journal of Computational Physics*, 392, 385–402.
- Papadrakakis, M., Papadopoulos, V., and Lagaros, N. D. (1996). “Structural reliability analysis of elastic-plastic structures using neural networks and monte carlo simulation.” *Computer Methods in Applied Mechanics and Engineering*, 136(1), 145–163.
- Rasmussen, C. E. and Williams, C. K. I. (2005). *Gaussian Processes for Machine Learning*. MIT Press.
- Schöbi, R. and Sudret, B. (2014). “Combining polynomial chaos expansions and kriging for solving structural reliability problems.” *7th Computational Stochastic Mechanics Conference*.
- Xu, J., Li, L., and Lu, Z. (2022). “An adaptive mixture of normal-inverse gaussian distributions for structural reliability analysis.” *Journal of Engineering Mechanics*, 148(3), 04022011.
- Zhang, C., Song, C., and Shafieezadeh, A. (2022). “Adaptive reliability analysis for multi-fidelity models using a collective learning strategy.” *Structural Safety*, 94.